JACS
JOURNAL OF THE AMERICAN CHEMICAL SOCIETY
Article
pubs.acs.org/JACS

Energetic Basis of Uncoupling Folding from Binding for an Intrinsically Disordered Protein

Igor Drobnak,[†,∥] Natalie De Jonge,[‡,§,⊥] Sarah Haesaerts,[‡,§] Gorazd Vesnaver,[†] Remy Loris,*[,‡,§] and Jurij Lah*[,†]

[†]Department of Physical Chemistry, Faculty of Chemistry and Chemical Technology, University of Ljubljana, Askerceva 5, 1000 Ljubljana, Slovenia

[‡]Molecular Recognition Unit, Department of Structural Biology, VIB, Pleinlaan 2, B-1050 Brussel, Belgium

[§]Structural Biology Brussels, Department of Biotechnology, Vrije Universiteit Brussel, Pleinlaan 2, B-1050 Brussel, Belgium

Supporting Information

ABSTRACT: Intrinsically disordered proteins (IDPs) are proteins that lack a unique three-dimensional structure in their native state. Many have, however, been found to fold into a defined structure when interacting with specific binding partners. The energetic implications of such behavior have been widely discussed, yet experimental thermodynamic data is scarce. We present here a thorough thermodynamic and structural study of the binding of an IDP (antitoxin CcdA) to its molecular target (gyrase poison CcdB). We show that the binding-coupled folding of CcdA is driven by a combination of specific intramolecular interactions that favor the final folded structure and a less specific set of intermolecular contacts that provide a desolvation entropy boost. The folded structure of the bound IDP appears to be defined largely by its own amino acid sequence, with the binding partner functioning more as a facilitator than a mold to conform to. On the other hand, specific intermolecular interactions do increase the binding affinity up to the picomolar range. Overall, this study shows how an IDP can achieve very strong and structurally well-defined binding and it provides significant insight into the molecular forces that enable such binding properties.

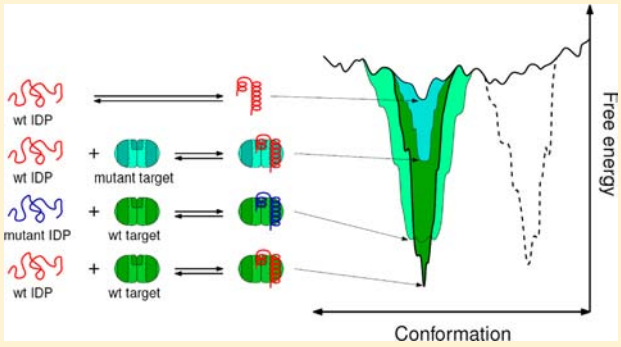

INTRODUCTION

Intrinsically disordered proteins[1−3] are a large and important class of proteins. On the basis of their amino acid contents and sequences, which differ considerably from globular proteins, they have been found to represent as much as 17% of proteins encoded in some eukaryotic genomes with up to 60% of proteins containing a disordered segment of at least 30 amino acids.[4,5] IDPs are also encoded in prokaryotic genomes, albeit with lower frequency. They function primarily in cell signaling and transcription regulation, but are conspicuously absent among enzymes.[6,7] Some IDPs function as permanently disordered entropic chains or linkers. Others exhibit enhanced binding to other biomolecules, as intrinsic disorder allows them to associate faster, to reach into more constrained spaces, to bind with a larger binding surface per residue, and in some cases to adapt their shape to bind to multiple different targets.[2,3,8,9] For a widespread group of IDPs, partner recognition is mediated by segments termed MoRFs (molecular recognition features) that undergo a disorder-to-order transition on binding. Due to the entropic penalty incurred on folding, it has been proposed that such proteins are able to uncouple binding specificity from affinity, resulting in binding that is highly specific without being too tight to be sensitive to small changes in cellular conditions.[1,2,9−11] Structures of IDP−target complexes have shown a remarkable diversity in the binding modes of IDPs: some remain completely unstructured, forming only transient intermolecular contacts, while others fold into well-defined structures that may be either encoded in their primary sequence or plastically adapted to the shape of the target molecule.[12−16]

Much work has been done to characterize IDPs both theoretically and experimentally.[3,17] Yet for a group of proteins whose functional properties depend largely on thermodynamics, there has been remarkably little detailed thermodynamic data[18] to substantiate the theoretical proposals about IDP behavior. We aim to offset this disparity by presenting here a thermodynamic and structural characterization of the intrinsically disordered domain of antitoxin CcdA that neutralizes the gyrase poison CcdB.

CcdA and CcdB constitute a toxin−antitoxin module, a bacterial system that functions in programmed cell death and/or stress response.[19−21] Previous characterization of the proteins involved and their interactions by us and other

Received: May 25, 2012
Published: January 4, 2013

groups[22−29] enables us to perform a detailed structural and thermodynamic investigation of this system. The interaction between the intrinsically disordered C-terminal domain of CcdA (CcdA$^{37-72}$, corresponding to Arg37−Trp72) and CcdB is of particular interest. Functionally, because it rejuvenates CcdB-poisoned gyrase−DNA complexes and facilitates autoregulation of the *ccd* operon.[29] More fundamentally, it represents an interesting case of extremely tight binding of an IDP to a given target, accompanied by its folding into an α-helical structure.

MATERIALS AND METHODS

Protein Preparation. In addition to the peptide CcdA$^{37-72}$ and dimeric protein $CcdB_2$, fragments of CcdB's target gyrase were used in this study. $GyrA14_2$ denotes a dimeric (2 × 14 kDa) fragment of the gyrase A subunit, which includes most of the $CcdB_2$ binding site, while the larger (2 × 59 kDa) fragment $GyrA59_2$ encompasses the entire binding site at the expense of slow in vitro binding kinetics. Procedures for the expression and isolation of $CcdB_2$, $GyrA14_2$, and $GyrA59_2$ have all been described previously.[30−32] The CcdA$^{37-72}$ peptide and its mutants were obtained from Bio-Synthesis (Lewisville, TX). The concentrations given below refer to the dimers of all three dimeric proteins ($CcdB_2$, $GyrA14_2$, $GyrA59_2$) whereas the concentrations of the monomeric CcdA$^{37-72}$ peptide are in monomer equivalents.

CD Spectroscopy. CD spectra were measured for unbound CcdA$^{37-72}$ and its mutants, as well as for unbound $CcdB_2$ and the corresponding CcdA$^{37-72}$:$CcdB_2$ (1:1) mixtures. The measurements were carried out on an Aviv 62A DS CD spectrophotometer (Aviv Associates, NJ), in the range 200−250 nm, using a spectral bandwidth of 2 nm and an averaging time of 2 s for the collection of each data point. The optical path length was 1 mm and the temperature was 25 °C. The secondary structure content was estimated using the three algorithms included in the CDPro package:[33] SELCON3, CDSSTR, and CONTIN-LL. We also tried the original version of CONTIN[34] and a linear combination of the reference spectra for pure secondary structures from Reed and Reed.[35]

X-ray Crystallography. Crystallization of the $CcdB_{2,Vf}$:CcdA$^{37-72}$ has been described before.[36] Data were collected at EMBL beamline X13 of the DESY synchrotron (Hamburg, Germany). Data collection statistics are given in Supplementary Table 1 (Supporting Information). The structure was determined by molecular replacement using PDB entry 3JRZ[37] as a search model. Phaser was able to place two $CcdB_{Vf}$ monomers in the atomic unit and clear electron density was visible for the missing CcdA$^{37-72}$ peptide. The structure was initially refined using Refmac at the initial stages and Phenix.refine near the end of the refinement. Model building was done using Coot. The final structure displays good geometries and final values of 0.1923 and 0.2524 for R_{work} and R_{free}, respectively. Full refinement statistics are given in Supplementary Table 1 (Supporting Information).

Experimental Binding Studies. Prior to isothermal calorimetric titration (ITC) all samples were dialyzed against 20 mM Tris-HCl buffer, pH 7.5, containing 150 mM NaCl and 1 mM EDTA. After dialysis their concentrations were determined from their measured UV absorbance at 280 nm and from their extinction coefficients (calculated according to Pace et al.[38]). The titrations were performed in a VP-ITC microcalorimeter (MicroCal, CT) using cell concentrations around 2−3 μM and injection syringe concentrations around 10−20 times higher. Several complete titrations were repeated in the corresponding phosphate buffer. The obtained ITC curves were the same as those measured in Tris buffer, indicating that no protonation/deprotonation is coupled to the measured association events.[39] The titration curves were analyzed by fitting a model function based on the mechanism in Figure 1 to experimental data using our own C++ fitting program. Details on the model fitting are available in the Supporting Information.

Structure-Based Thermodynamic Calculations. The contributions from folding and binding were estimated from the CcdA$^{37-72}$−$CcdB_2$ complex structure[29] (PDB ID 3HPW) using empirical structure−thermodynamics relations.[40,41] In addition to the final complex structure, the calculation requires the solvent accessible surface areas of other protein species. The structures of a folded but unbound CcdA$^{37-72}$ and an unbound $CcdB_2$ were generated by deleting the other molecule from the complex structure. The structure of unfolded CcdA$^{37-72}$ was approximated by the sum of contributions from AXA tripeptides with X running over all amino acids in CcdA$^{37-72}$. While this is not an accurate representation of the actual structure of unfolded CcdA$^{37-72}$, it is the method used to parametrize the empirical structure−thermodynamics relationships,[42] and its use compensates for some of the bias in the parametrized equations. Further details on the calculation are presented in the Supporting Information.

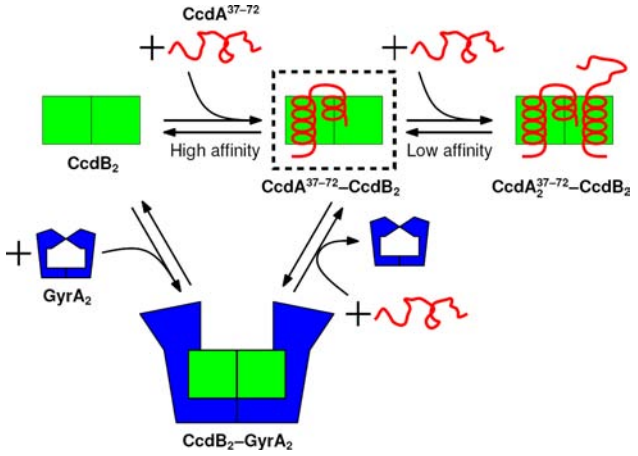

Figure 1. Equilibrium model of the system used to determine the thermodynamics of CcdA$^{37-72}$−CcdB binding. Direct binding of the intrinsically disordered antitoxin CcdA$^{37-72}$ (red) to the toxin $CcdB_2$ (green) is too strong to enable direct determination of the binding constant. Therefore, $CcdB_2$ was first bound to its cellular target, $GyrA_2$ (blue). The subsequent addition of CcdA$^{37-72}$ displaces $GyrA_2$ and results in the formation of the high-affinity CcdA$^{37-72}$−$CcdB_2$ complex (dashed box). A second CcdA$^{37-72}$ can also bind with a lower affinity.

RESULTS

Determination of CcdA−CcdB Binding Thermodynamics. Previous studies have suggested that CcdA$^{37-72}$ recognizes CcdB with an affinity in the picomolar range[29]—very high given that some of the strongest known IDP−target interactions are in the low nanomolar range.[43−45] In order to obtain insight into the origin of this high affinity, the associated thermodynamic parameters were obtained by global model analysis of isothermal titration calorimetry (ITC) data measured for the protein−protein interacting system at different temperatures. Due to the very high binding affinity of CcdA$^{37-72}$ for CcdB, we were not able to determine the binding thermodynamics from direct titrations alone. The problem was circumvented by measuring ITC titration curves for the binding of CcdB to its target, DNA gyrase (GyrA), and then titrating the CcdB−GyrA complex with CcdA$^{37-72}$, which releases GyrA and produces a CcdA$^{37-72}$−CcdB complex. Additional complications to this system include the fact that both CcdB and GyrA are dimers and that the size of $GyrA_2$ makes it difficult to work with in vitro, so two different truncation mutants ($GyrA14_2$ and $GyrA59_2$, see Supporting Information for details) were used in the actual titrations. There is also an additional low-affinity binding step where a second CcdA$^{37-72}$ molecule binds to an existing CcdA$^{37-72}$−$CcdB_2$ complex, forming CcdA$^{37-72}{}_2$−$CcdB_2$. An equilibrium model describing the entire system (Figure 1) was fitted to the

dx.doi.org/10.1021/ja305081b | J. Am. Chem. Soc. 2013, 135, 1288−1294

data from all titrations using a global approach[46] to obtain thermodynamic parameters for each binding reaction. The model is based on previous knowledge about the *ccd* toxin–antitoxin system[24−29] and describes the experimental ITC data very well (Supplementary Figure 2, Supporting Information). The present work focuses on the formation of the high-affinity $CcdA^{37-72}$–$CcdB_2$ complex (dashed box in Figure 1), but the thermodynamics of other reactions can be found in Supplementary Table 3 (Supporting Information).

Origin of the High Affinity between CcdA and CcdB. $CcdA^{37-72}$ is intrinsically disordered by itself as well as in the context of the full-length $CcdA_2$, which includes a folded N-terminal dimerization domain, as shown by the NMR structure.[27] This is not surprising, given its low hydrophobicity (−1.26 average hydropathy on the Kyte–Doolittle scale[47]) and high charge (15 out of 36 residues are charged). To get from this disordered state to the helical conformation seen in the structure of the $CcdA^{37-72}$–$CcdB_2$ complex,[29] binding needs to be accompanied by $CcdA^{37-72}$ folding. To better understand this phenomenon, we performed a dissection of the standard thermodynamic parameters of $CcdA^{37-72}$–$CcdB_2$ complex formation (ΔF°) into contributions due to $CcdA^{37-72}$ folding (ΔF°_{fold}) and binding of the prefolded $CcdA^{37-72}$ to $CcdB_2$ (ΔF°_{bind}):

$$\Delta F^\circ = \Delta F^\circ_{fold} + \Delta F^\circ_{bind}; \quad F = G, H, S, C_p \qquad (1)$$

where G, H, S, and C_p represent Gibbs free energy, enthalpy, entropy, and heat capacity, respectively. The two contributions to each thermodynamic quantity (F) were estimated using empirical parametrizations[40,41] that are mainly based on changes in solvent-accessible surface areas. Note that the mechanism (folding of $CcdA^{37-72}$ + binding of prefolded $CcdA^{37-72}$; see eq 11 in Supporting Information) used for the dissection (eq 1) is entirely theoretical and there is no experimental evidence to distinguish between the mechanisms of conformational selection (folding followed by binding), induced folding (binding followed by folding), or anything in between. The choice of the presented model for the dissection is based on the availability of the structural data required for the calculation (it is easier to construct a structure of a folded unbound $CcdA^{37-72}$ than of an unfolded $CcdA^{37-72}$ bound to $CcdB_2$). On the other hand, the validity of the dissection does not depend on the actual mechanism, since all the discussed thermodynamic quantities (ΔF°) are state functions.

The results (Figure 2a and Supplementary Table 5, Supporting Information) suggest that the observed high affinity of $CcdA^{37-72}$ for its target is achieved by a combination of a highly favorable enthalpy of $CcdA^{37-72}$ folding into an α-helical structure and a favorable entropy contribution due to burial of the large, mostly hydrophobic surface areas forming the binding interface. Together, these two contributions overcome the large loss of conformational entropy associated with $CcdA^{37-72}$ folding. In this regard, the binding–coupled folding of $CcdA^{37-72}$ can be seen as analogous to the folding of globular proteins, which is driven by a similar balance of forces.

Mutations of Noncontacting Residues Modulate the Nature of Binding-Induced Folding. To investigate the effect of $CcdA^{37-72}$ folding properties on complex formation, we designed four mutant peptides, termed poly-Ala, poly-Glu, poly-Gly, and poly-Thr. In these mutants, all residues in the segment Arg40–Gly63 whose side chains remain solvent exposed upon interaction with $CcdB_2$ were substituted by Ala, Glu, Gly, or Thr, respectively (Figure 3a; see

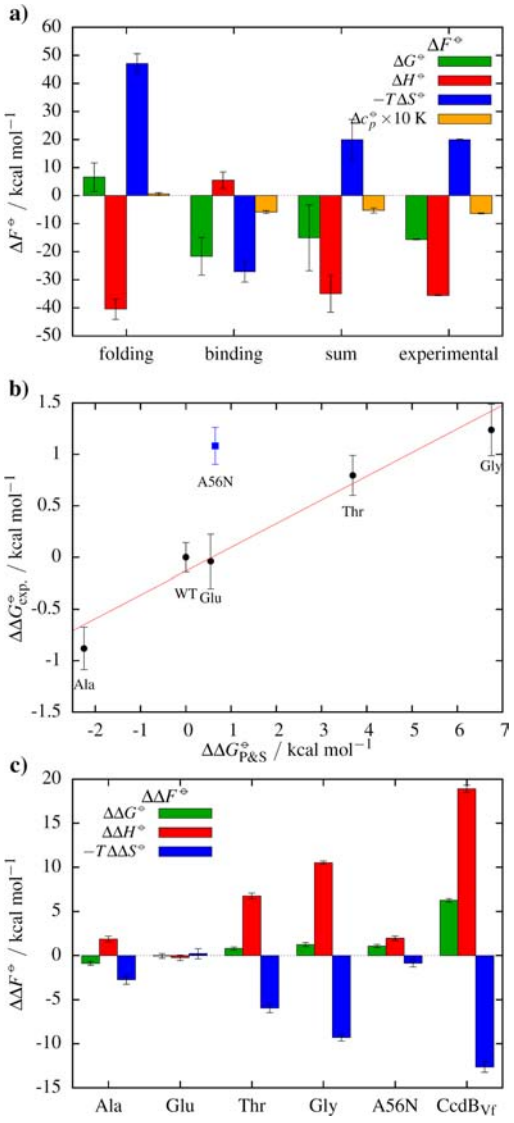

Figure 2. Thermodynamics of $CcdA^{37-72}$–$CcdB_2$ association. (a) Dissection of wild-type thermodynamics into hypothetical contributions of folding $CcdA^{37-72}$ in the absence of $CcdB_2$ and of binding a prefolded $CcdA^{37-72}$ to $CcdB_2$. The contributions were calculated using empirical relations between structural features and thermodynamic parameters.[40,41] (b) Effect of $CcdA^{37-72}$ mutations on the free energy of binding to $CcdB_2$, compared to the wild-type peptide. Ala, Glu, Thr, and Gly denote the respective poly-Xxx $CcdA^{37-72}$ mutants. The experimental values ($\Delta\Delta G^\circ_{exp}$) correlate well with the predictions based on the helix propensity scale of Pace and Scholtz[48] ($\Delta\Delta G^\circ_{P\&S}$), except for the contacting residue mutant, labeled "A56N" and shown in blue. (c) Effects of mutations on the thermodynamics of binding, compared to wild-type. $CcdB_{2,Vf}$ denotes the binding of $CcdA^{37-72}$ to the noncognate $CcdB_{2,Vf}$.

Supplementary Table 2, Supporting Information for sequences). The resulting peptides differ from wild-type in their α-helix propensities[48,49] while the same binding interface are maintained. Circular dichroism (CD) spectra (Figure 3b) show that in the absence of $CcdB_2$ all the tested peptides remain largely unstructured. By contrast, in complex with $CcdB_2$, the CD spectra of all peptides indicate a significant degree of α-helical structure. Interestingly, the bound state mutant peptides exhibit significantly lower degrees of helicity than the wild-type. Quantitative analysis of the CD spectra confirms these findings

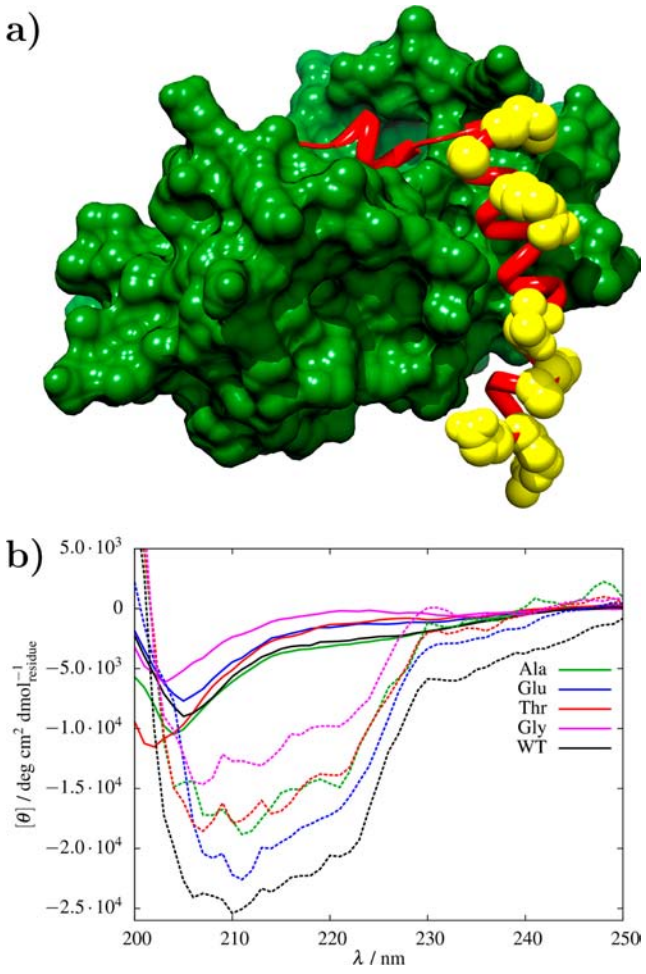

Figure 3. Structural properties of $CcdA^{37-72}$ mutants. (a) Crystal structure of $CcdA^{37-72}$ (red) in complex with $CcdB_2$ (green) presented using UCSF Chimera.[50] The mutated noncontacting amino acids are highlighted in yellow. Sequences of all mutants are given in Supplementary Table 2 (Supporting Information). (b) Normalized CD spectra of $CcdA^{37-72}$ and its mutant variants, free and in complex with $CcdB_2$. Full lines correspond to the unbound form, while the dashed lines represent the folded form and were obtained by subtracting the contribution of unbound $CcdB_2$ from spectra of $CcdA^{37-72}$–$CcdB_2$ complexes. The latter are much more noisy because they are difference spectra.

but does not give reliable absolute estimates of secondary structure content (see the Supporting Information for details).

The effects of mutations on the binding affinity correlate well with the values predicted from the helix-propensity scale of Pace and Scholtz[48] (Figure 2b and Supplementary Table 4, Supporting Information), suggesting that the changes in affinity are largely due to the altered folding properties of the mutants. The experimental $\Delta\Delta G^\circ$ values ($\Delta\Delta G^\circ = \Delta G^\circ_{mutant} - \Delta G^\circ_{wild\text{-}type}$) account for about 25% of the predicted value, which may be in large part explained by $CcdA^{37-72}$ having more than 0% helical content in the unbound state and less than 100% in the complex (the changes in helicity calculated from CD spectra are in the 10–60% range, depending on the algorithm and set of reference spectra used). To support the hypothesis that mutations of noncontacting residues influence $CcdA^{37-72}$–$CcdB_2$ association predominantly through $CcdA^{37-72}$ folding, we performed control binding experiments with several mutant peptides that involve a point mutation of a (contacting) residue located in the $CcdA^{37-72}$–$CcdB_2$ binding interface. Binding of these mutant peptides to $CcdB_2$ results in $\Delta\Delta G^\circ$ values that are significantly more positive than would be expected based only on helix propensity. This demonstrates that mutations of contacting residues introduce an additional contribution to the thermodynamics of association, separate from that seen with mutations of noncontacting residues. Such a result is expected if contacting residues affect both folding and binding properties of the peptide, while noncontacting residues predominantly influence folding. Data for a representative contacting mutant, A56N, is presented here for comparison to noncontacting mutants (Figure 2 and Supplementary Tables 2 and 4 and Supplementary Figure 4f, Supporting Information).

All the measured noncontacting mutant peptides also show a higher (less favorable) enthalpy and higher (less unfavorable) entropy of binding compared to wild-type (positive $\Delta\Delta H^\circ$ and $\Delta\Delta S^\circ$ values in Figure 2c). Such a thermodynamic profile and the observed lower helical content of mutant peptides in the complex suggest that the mutations are disrupting favorable interactions that hold several amino acids and/or water molecules firmly in place in the $CcdB_2$-bound structure. This interpretation is further supported by our structure-based dissection of $CcdA^{37-72}$–$CcdB_2$ binding thermodynamics (Figure 2a and Supplementary Table 5, Supporting Information), which emphasizes the profound impact the folding properties of the MoRF can have on the overall energetics of association.

CcdA Does Not Adapt Its Structure to the Recognition Surface of Its Partner. The specificity/affinity uncoupling model[1,2,11] implicitly assumes that the IDP would not adapt its structure to that of a nonidentical but related binding surface on a different partner or that such a structural adaptation requires a distortion that is energetically unfavorable. This assumption is intuitively in contrast with the ability to bind multiple partners and was tested by examining the interaction between F-plasmid $CcdA_F^{37-72}$ and a $CcdB_2$ protein encoded in the genome of *Vibrio fischeri* ($CcdB_{2,Vf}$). $CcdB_{2,Vf}$ and $CcdB_{2,F}$ share 41% sequence identity, which reduces to 37% when only the residues constituting the binding site are considered. Similarly, the C-terminal domains of the two corresponding CcdAs share only 19% sequence identity. Replacing $CcdB_{2,F}$ with $CcdB_{2,Vf}$ therefore significantly changes the binding interface without changing the folding properties of the IDP itself. ITC measurements show that the affinity between $CcdA_F^{37-72}$ and $CcdB_{2,Vf}$ is in the micromolar range. The large (5 orders of magnitude) drop in affinity is due to a large enthalpic penalty associated with the mismatch of surfaces, which is only partially compensated by a gain in entropy (Figure 2c and Supplementary Table 4, Supporting Information). This is explained by the crystal structure of $CcdB_{2,Vf}$ in complex with $CcdA_F^{37-72}$, which shows little if any difference in the $CcdA_F^{37-72}$ backbone conformation when binding to the two different partners (Figure 4a). Likewise, side chains typically adopt the same rotamer conformation in both complexes. The most conspicuous difference is the poorer definition of a number of $CcdA_F^{37-72}$ side chains in the complex with $CcdB_{2,Vf}$. Thus, rather than folding into an alternative structure, those side chains that are prevented from adopting the same conformation as in the complex with $CcdB_{2,F}$ remain frustrated and fail to adopt a unique conformation. The similarities in the bound conformations of $CcdA_F^{37-72}$ are

dx.doi.org/10.1021/ja305081b | J. Am. Chem. Soc. 2013, 135, 1288–1294

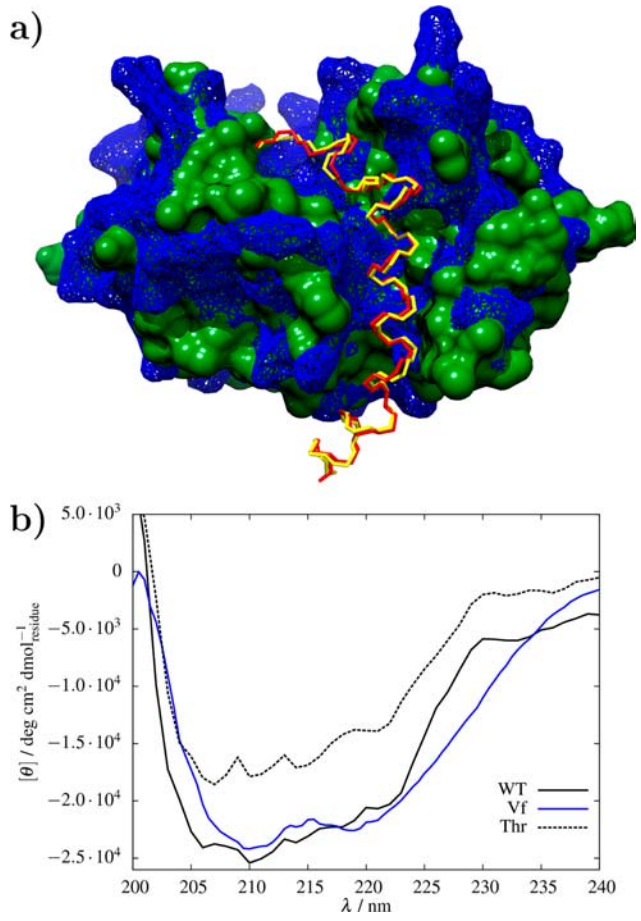

Figure 4. Effect of binding partner on the $CcdA^{37-72}$ structure. (a) Superposition of the crystal structures of $CcdA^{37-72}{}_F$–$CcdB_{2,F}$ (in red and green, respectively) and $CcdA^{37-72}{}_F$–$CcdB_{2,Vf}$ (in yellow and blue, respectively) complexes presented using UCSF Chimera.[50] The conformation of the $CcdA^{37-72}{}_F$ backbone is nearly identical in both complexes. (b) Normalized CD spectra of $CcdA^{37-72}$ in complex with $CcdB_{2,F}$ (WT, black) and $CcdB_{2,Vf}$ (Vf, blue) obtained by subtracting the contribution of unbound $CcdB_2$ from spectra of $CcdA^{37-72}$–$CcdB_2$ complexes. The spectrum of poly-Thr $CcdA^{37-72}$ in complex with $CcdB_{2,F}$ (Thr, dashed black line) is also plotted for comparison.

further emphasized by the CD spectra of both complexes, where the contributions of $CcdA_F^{37-72}$ are very similar (Figure 4b).

DISCUSSION

The $CcdA^{37-72}$–$CcdB_2$ complex has a specific, well-defined structure; this cannot be considered as a unique property, but neither it is self-evident, since there is strong experimental evidence that many IDPs can form partially flexible ("fuzzy") complexes.[16] The structure is stabilized by a low enthalpy of folding (given that any mutations increase the enthalpy) and the entropy contribution of the hydrophobic effect from binding. Specific side-chain interactions with $CcdB_2$ greatly enhance the binding affinity (by 5 orders of magnitude), but even so their absence does not affect the structure of the $CcdA_F^{37-72}$–$CcdB_{2,Vf}$ complex. Considering that $CcdA^{37-72}$ folds correctly even in the presence of $CcdB_{2,Vf}$, it is reasonable to conclude that specific side-chain interactions with the binding partner do not determine the folded structure of $CcdA^{37-72}$. Yet, a binding partner is necessary to facilitate folding (since $CcdA^{37-72}$ is unfolded in the absence of a binding partner; Figure 3b). We therefore suggest that it is the general shape of the binding site with an appropriate hydrophobic character that induces the binding-coupled folding of $CcdA^{37-72}$. Our results are thus in agreement with the suggestion that nonspecific hydrophobic interactions facilitate MoRF folding,[15] yet they also indicate that specific side-chain interactions contribute importantly to the affinity.

We have shown that mutations in the noncontacting residues of $CcdA^{37-72}$ (which change the folding properties, but not the binding interface) affect the structure of the complex (Figure 3). On the other hand, mutations in the binding interface of the target molecule (which do not change the folding properties of $CcdA^{37-72}$) have a much smaller effect on the complex structure (Figure 4). This suggests that the amino acid sequence (including noncontacting residues) of $CcdA^{37-72}$ is more important for determining the folded structure than the specific contacts it finds in the binding interface. This is in accordance with previous theoretical suggestions[11−13] that the secondary structure MoRFs assume on binding is already encoded in their amino acid sequence. We should point out, however, that the

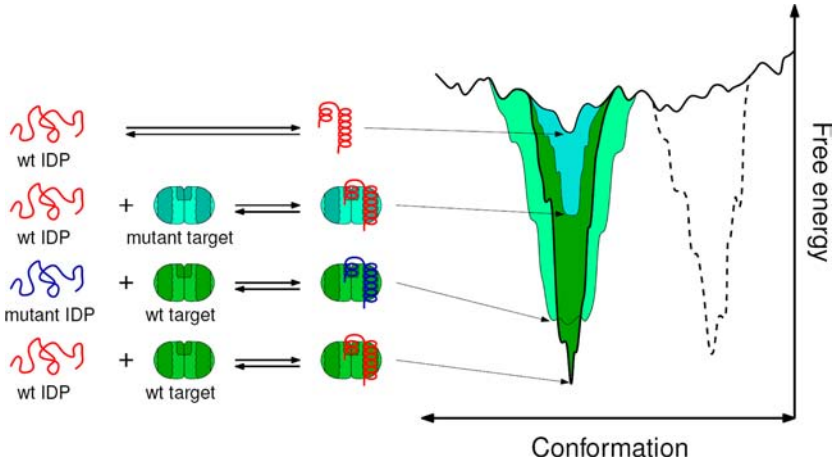

Figure 5. Schematic representation of the proposed shape of the conformational free energy landscape (folding funnel) of $CcdA^{37-72}$. The narrow minimum represents the folded conformation, which is stabilized by interactions with $CcdB_2$ and destabilized by mutations in the IDP or its target. The dashed line shows a hypothetical second folded conformation that would allow binding to a different target.

dx.doi.org/10.1021/ja305081b | J. Am. Chem. Soc. 2013, 135, 1288−1294

presence of an appropriate binding partner is necessary to "unlock" this preferred structure—the MoRF on its own remains disordered.

Our view of the folding properties of $CcdA^{37-72}$ can be presented in terms of a folding funnel schematic,[51−53] shown in Figure 5. On its own, the IDP is unfolded, without a distinct free energy minimum. In the presence of a binding partner with a correct general shape and hydrophobicity of the binding site, the free energy landscape changes; favorable interactions with the binding partner stabilize the specific α-helical conformation, forming a folding funnel in the free energy landscape.[54] The free energy minimum can be further deepened by specific, finely tuned, side-chain interactions such as exist between $CcdA_F^{37-72}$ and $CcdB_{2,F}$, but not between $CcdA_F^{37-72}$ and $CcdB_{2,Vf}$. On the other hand, mutations in the IDP can change its intrinsic propensity for the specific folded conformation, widening the folding funnel so that a wider range of conformations may be explored even in the presence of a binding partner.

The encoding of preferred MoRF conformations in the primary sequence need not be incompatible with binding to multiple partners. Metamorphic globular proteins display several distinct conformations in equilibrium under physiological conditions, with different conformers forming complexes with different ligands.[55] Similar behavior is even more prevalent in IDPs.[56,57] This may be explained by interactions with each of the different binding partners stabilizing one of several pre-encoded (preferred) conformations by deepening its local minimum in the free energy landscape (Figure 5). This mode of IDP interaction is an extension of the classical structure−function paradigm and is distinct from the concept of fuzzy complexes, where IDPs engage in transient interactions with limited or no associated folding.[16]

■ CONCLUSIONS

Intrinsically disordered proteins represent an exciting field of research that challenges our understanding of protein structure and functioning. There appears to be great diversity in the binding affinities and the degrees of flexibility retained by IDPs in complexes with binding partners. This study highlights one of the ways an IDP's structure can be influenced by its binding partner to unlock a specific, low-energy functional state. Other classes of IDPs may well use different mechanisms, and thus, more thermodynamic and structural studies will be needed to gain a better insight into the driving forces of binding-coupled folding. Hopefully, this approach will lead to better understanding of the behavior of unstructured proteins and their cellular functions.

■ ASSOCIATED CONTENT

Ⓢ Supporting Information

Methods: Model analysis of data, structure-based thermodynamic calculations, analysis of CD spectra, and table of peptide sequences. Results: Figures and tables describing ITC and X-ray crystallography experiments. This material is available free of charge via the Internet at http://pubs.acs.org.

■ AUTHOR INFORMATION

Corresponding Author

remy.loris@vib-vub.be; jurij.lah@fkkt.uni-lj.si

Present Addresses

[‖]Department of Chemistry and Biochemistry, University of Notre Dame, 251 Niewland Science Hall, Notre Dame, Indiana 46556−5670.

[⊥]arGEN-X, Technologiepark 30, B-9052 Zwijnaarde, Belgium.

Notes

The authors declare no competing financial interest.

■ ACKNOWLEDGMENTS

We thank Mario Šimić and Lieven Buts for performing some preliminary binding experiments, Andrej Mernik for titrations of contacting mutants, as well as Prof. Peter Tompa and Prof. Roger Pain for a critical reading of the manuscript. This work was supported by grants from the Ministry of Higher Education, Science and Technology, and the Agency for Research of Republic of Slovenia, the Fonds voor Wetenschappelijk Onderzoek (FWO) Vlaanderen, the Onderzoeksraad of the Vrije Universiteit Brussel, and the Vlaams Interuniversitair Instituut voor Biotechnologie. N.D.J. received a predoctoral grant from the Instituut voor Wetenschap en Technologie (IWT) and R.L. received from "the Hercules Foundation".

■ REFERENCES

(1) Wright, P. E.; Dyson, H. J. *J. Mol. Biol.* **1999**, *293*, 321−331.
(2) Tompa, P. *Trends Biochem. Sci.* **2002**, *27*, 527−533.
(3) Uversky, V. N.; Dunker, A. K. *Biochim. Biophys. Acta* **2010**, *1804*, 1231−1264.
(4) Ward, J.; Sodhi, J.; McGuffin, L.; Buxton, B.; Jones, D. *J. Mol. Biol.* **2004**, *337*, 635−645.
(5) Oldfield, C. J.; Cheng, Y.; Cortese, M. S.; Brown, C. J.; Uversky, V. N.; Dunker, A. K. *Biochemistry* **2005**, *44*, 1989−2000.
(6) Dyson, H. J.; Wright, P. E. *Nat. Rev. Mol. Cell Biol.* **2005**, *6*, 197−208.
(7) Fuxreiter, M.; Tompa, P.; Simon, I.; Uversky, V. N.; Hansen, J. C.; Asturias, F. J. *Nat. Chem. Biol.* **2008**, *4*, 728−737.
(8) Dunker, A. K.; Brown, C. J.; Lawson, J. D.; Iakoucheva, L. M.; Obradović, Z. *Biochemistry* **2002**, *41*, 6573−6582.
(9) Chen, J. *J. Am. Chem. Soc.* **2009**, *131*, 2088−2089.
(10) Spolar, R.; Record, J. M. T. *Science* **1994**, *263*, 777−784.
(11) Oldfield, C. J.; Cheng, Y.; Cortese, M. S.; Romero, P.; Uversky, V. N.; Dunker, A. K. *Biochemistry* **2005**, *44*, 12454−12470.
(12) Mohan, A.; Oldfield, C. J.; Radivojac, P.; Vacic, V.; Cortese, M. S.; Dunker, A. K.; Uversky, V. N. *J. Mol. Biol.* **2006**, *362*, 1043−1059.
(13) Fuxreiter, M.; Simon, I.; Friedrich, P.; Tompa, P. *J. Mol. Biol.* **2004**, *338*, 1015−1026.
(14) Mészáros, B.; Tompa, P.; Simon, I.; Dosztányi, Z. *J. Mol. Biol.* **2007**, *372*, 549−561.
(15) Vacic, V.; Oldfield, C. J.; Mohan, A.; Radivojac, P.; Cortese, M. S.; Uversky, V. N.; Dunker, A. K. *J. Proteome Res.* **2007**, *6*, 2351−2366.
(16) Tompa, P.; Fuxreiter, M. *Trends Biochem. Sci.* **2008**, *33*, 2−8.
(17) Sugase, K.; Dyson, H. J.; Wright, P. E. *Nature* **2007**, *447*, 1021−1025.
(18) Ferreon, J. C.; Hilser, V. J. *Biochemistry* **2004**, *43*, 7787−7797.
(19) Buts, L.; Lah, J.; Dao-Thi, M.-H.; Wyns, L.; Loris, R. *Trends Biochem. Sci.* **2005**, *30*, 672−679.
(20) Gerdes, K.; Christensen, S. K.; Lobner-Olesen, A. *Nat. Rev. Microbiol.* **2005**, *3*, 371−382.
(21) Van Melderen, L.; Saavedra De Bast, M. *PLoS Genet.* **2009**, *5*, e1000437.
(22) Critchlow, S. E.; O'Dea, M. H.; Howells, A. J.; Couturier, M.; Gellert, M.; Maxwell, A. *J. Mol. Biol.* **1997**, *273*, 826−839.
(23) Loris, R.; Dao-Thi, M.-H.; Bahassi, E. M.; Melderen, L. V.; Poortmans, F.; Liddington, R.; Couturier, M.; Wyns, L. *J. Mol. Biol.* **1999**, *285*, 1667−1677.

(24) Afif, H.; Allali, N.; Couturier, M.; Van Melderen, L. *Mol. Microbiol.* **2001**, *41*, 73−82.
(25) Dao-Thi, M.-H.; Charlier, D.; Loris, R.; Maes, D.; Messens, J.; Wyns, L.; Backmann, J. *J. Biol. Chem.* **2002**, *277*, 3733−3742.
(26) Dao-Thi, M.-H.; Melderen, L. V.; Genst, E. D.; Afif, H.; Buts, L.; Wyns, L.; Loris, R. *J. Mol. Biol.* **2005**, *348*, 1091−1102.
(27) Madl, T.; van Melderen, L.; Mine, N.; Respondek, M.; Oberer, M.; Keller, W.; Khatani, L.; Zangger, K. *J. Mol. Biol.* **2006**, *364*, 170−185.
(28) Šimić, M.; de Jonge, N.; Loris, R.; Vesnaver, G.; Lah, J. *J. Biol. Chem.* **2009**, *284*, 20002−20010.
(29) De Jonge, N.; Garcia-Pino, A.; Buts, L.; Haesaerts, S.; Charlier, D.; Zangger, K.; Wyns, L.; de Greve, H.; Loris, R. *Mol. Cell* **2009**, *35*, 154−163.
(30) Buts, L.; De Jonge, N.; Loris, R.; Wyns, L.; Dao-Thi, M.-H. *Acta Crystallogr. Sect. F* **2005**, *61*, 949−952.
(31) Dao-Thi, M.-H.; Van Melderen, L.; De Genst, E.; Buts, L.; Ranquin, A.; Wyns, L.; Loris, R. *Acta Crystallogr. Sect. D* **2004**, *60*, 1132−1134.
(32) Reece, R. J.; Maxwell, A. *J. Biol. Chem.* **1991**, *266*, 3540−3546.
(33) Sreerama, N.; Woody, R. W. *Anal. Biochem.* **2000**, *287*, 252−260.
(34) Provencher, S. W.; Gloeckner, J. *Biochemistry* **1981**, *20*, 33−37.
(35) Reed, J.; Reed, T. A. *Anal. Biochem.* **1997**, *254*, 36−40.
(36) De Jonge, N.; Buts, L.; Vangelooven, J.; Mine, N.; Van Melderen, L.; Wyns, L.; Loris, R. *Acta Crystallogr. Sect. F* **2007**, *63*, 356−360.
(37) De Jonge, N.; Hohlweg, W.; Garcia-Pino, A.; Respondek, M.; Buts, L.; Haesaerts, S.; Lah, J.; Zangger, K.; Loris, R. *J. Biol. Chem.* **2010**, *285*, 5606−5613.
(38) Pace, C. N.; Vajdos, F.; Fee, L.; Grimsley, G.; Gray, T. *Protein Sci.* **1995**, *4*, 2411−2423.
(39) Baker, B. M.; Murphy, K. P. *J. Mol. Biol.* **1997**, *268*, 557−569.
(40) Murphy, K. P.; Freire, E. *Adv. Protein Chem.* **1992**, *43*, 313−361.
(41) Xie, D.; Freire, E. *Proteins* **1994**, *19*, 291−301.
(42) Robertson, A. D.; Murphy, K. P. *Chem. Rev.* **1997**, *97*, 1251−1267.
(43) Kriwacki, R. W.; Hengst, L.; Tennant, L.; Reed, S. I.; Wright, P. E. *Proc. Natl. Acad. Sci. U. S. A.* **1996**, *93*, 11504−11509.
(44) Petros, A. M.; Nettesheim, D. G.; Wang, Y.; Olejniczak, E. T.; Meadows, R. P.; Mack, J.; Swift, K.; Matayoshi, E. D.; Zhang, H.; Fesik, S. W.; Thompson, C. B. *Protein Sci.* **2000**, *9*, 2528−2534.
(45) Dames, S. A.; Martinez-Yamout, M.; De Guzman, R. N.; Dyson, H. J.; Wright, P. E. *Proc. Natl. Acad. Sci. U. S. A.* **2002**, *99*, 5271−5276.
(46) Drobnak, I.; Vesnaver, G.; Lah, J. *J. Phys. Chem. B* **2010**, *114*, 8713−8722.
(47) Kyte, J.; Doolittle, R. F. *J. Mol. Biol.* **1982**, *157*, 105−132.
(48) Pace, C. N.; Scholtz, J. M. *Biophys. J.* **1998**, *75*, 422−427.
(49) Richardson, J. M.; Lopez, M. M.; Makhatadze, G. I. *Proc. Natl. Acad. Sci. U. S. A.* **2005**, *102*, 1413−1418.
(50) Pettersen, E. F.; Goddard, T. D.; Huang, C. C.; Couch, G. S.; Greenblatt, D. M.; Meng, E. C.; Ferrin, T. E. J. *Comput. Chem.* **2004**, *25*, 1605−1612.
(51) Dill, K. A. *Protein Sci.* **1999**, *8*, 1166−1180.
(52) Tsai, C.-J.; Kumar, S.; Ma, B.; Nussinov, R. *Protein Sci.* **1999**, *8*, 1181−1190.
(53) Onuchic, J. N.; Wolynes, P. G. *Curr. Opin. Struct. Biol.* **2004**, *14*, 70−75.
(54) Higo, J.; Nishimura, Y.; Nakamura, H. *J. Am. Chem. Soc.* **2011**, *133*, 10448−10458.
(55) Murzin, A. G. *Science* **2008**, *320*, 1725−1726.
(56) Tompa, P.; Szász, C.; Buday, L. *Trends Biochem. Sci.* **2005**, *30*, 484−489.
(57) Oldfield, C.; Meng, J.; Yang, J.; Yang, M. Q.; Uversky, V. N.; Dunker, A. K. *BMC Genomics* **2008**, *9*, S1.